Application of I-COMO Device towards Geographic Disease Enrichment Pattern Revealed from Electronic Medical Record at A Large Urban Academic Medical Center

Matteo Danieletto*
Institute for Next Generation Healthcare 770 Lexington Ave., New York, NY 10029
USA
matteo.danieletto@mssm.edu

Li Li*
Institute for Next Generation Healthcare 770 Lexington Ave., New York, NY 10029
USA
li.li@mssm.edu

Joel T. Dudley
Institute for Next Generation Healthcare 770 Lexington Ave., New York, NY 10029
USA
joel.dudley@mssm.edu

* Equal contributions

ABSTRACT

For decades, the air pollution has been studied as key driver factor for uncountable number of diseases ranging from respiratory diseases to neoplasms. However, in each city, the effort to control the air quality is low. Plenty of studies report the importance of quality of air, but majority of them is based on outdoors air quality that do not consider or track people outside or inside a building. In this study, we have analyzed the largest electronic medical records (EMR) in New York City and air pollution data collected from environmental protection agency (EPA) to identify environmental diseases impacted by air pollution. We have identified that the different environmental diseases are significantly enriched to certain geographic areas influenced by surrounding environment. Therefore, using this data-driven approach, we are here to present a new Internet of Things network concept. The new architecture based on LoRaWAN has the objective to bypass most of the issues encountered in these years to collect patient data as well as to improve the telemedicine. At the same time, the network can open new scenario of crowdsourcing to improve the granularity of data collection. Third-party companies can use IoT infrastructure to test new devices and to integrate the existing data sets.

KEYWORDS

Environmental diseases, Electronic medical records, IoT, LoRaWAN network, Air Pollution

1 INTRODUCTION

The World Health Organization (WHO) reports that an estimated 12.6 million deaths each year are attributable to unhealthy environments - nearly one in four of total global deaths. Environmental risk factors, such as air, water and soil pollution, chemical exposures, climate change and ultraviolet radiation, contribute to more than 100 diseases and injuries (http://www.who.int). The association between public health and the environment has been extensively studied and environmental risks have been proven to significantly impact human health. The concerns have often resulted in public observations of disease clusters near hazardous waste sites, air pollution caused by traffic, and other potential sources of chemical releases. United States Environmental Protection Agency (EPA) indicates that although levels of particle pollution and ground-level ozone pollution are substantially lower than in the past, there are still unhealthy levels in numerous areas of the country. Many studies have shown that the air pollution increases the risks of numerous diseases including respiratory disease, chronic kidney diseases, cancer, fertility problems, and heart diseases [1-3] [4, 5]. Identifying the risks of environmental diseases specifically to geographic regions and building a customized device has become an ultimate goal to measure the environmental factors at granular level unique to these regions.

The Internet of Things (IoT) paradigm has been defined recently to improve the quality of life and to gather more information of the world. In this new paradigm, every single object (animated and/or unanimated) can be part of Internet with the feature to exchange data without the human interaction. An example combining IoT and telemedicine is the work presented [6] where a patient with amyotrophic lateral sclerosis (ASL) was able to remotely control a robot through a Brain Computer Interface (BCI) P-300 wave. The self-autonomous robot was able to move in an indoor scenario exploiting the IoT network as peers to navigate.

Thus, telemedicine application, which combines wireless technology and any user interaction through the smartphones, could have a great impact to monitor a specific group of patients. With such network architecture, the human has the central role of the network, where the information is produced and consumed from a physical individual.

In this study, we analyzed the air pollution data reported from EPA and the largest comprehensive electronic medical record (EMR) [7] [8] in Mount Sinai Hospital (MSH), representing the New York City population and geographic diversity, involving 7 unique millions patients with 1.5 million unique patient diagnoses across thousands of zip codes coverage. We identified respiratory diseases are significantly enriched in east Harlem area, circulatory disease, metabolic diseases, immunity disorders are significantly enriched in upper Manhattan, while neoplasm and genitourinary disease are enriched in the midtown and upper west area. This is the first study to show the environmental diseases are affected and distributed in different areas in NYC. Additionally, we introduce a new IoT architecture based on LoRaWAN (https://www.lora-

PervasiveHealth '17, May 23–26, 2017, Barcelona, Spain

ACM ISBN 978-1-4503-6363-1/17/05…$15.00
https://doi.org/10.1145/3154862.3154913

alliance.org), which will be implemented in the future work and can improve the granularity of air pollution data both indoor and outdoor settings and bypass the most common problem to deploy a massive data collection campaign in order to improve the patient quality of life.

2 Medical Records dataset and LoRaWAN

2.1 Study design

The aim of our study was to apply a novel non-invasive device application in New York City (NYC) to better monitor and to understand the potential effects on environmental diseases on our diverse patient populations through a comprehensive data driven approach.

2.2 Patient population

We used electronic medical record (EMR) from our Mount Sinai Hospitals (MSH), one of the largest EMR in NYC, representing entire NYC patient population with diverse ethnicities including 36% Caucasian, 13% African American, 21% Hispanic and others [7]. The data collection frame was from Jan 2005 – May 2016 and we obtained 1,562,186 unique patients with disease diagnosis in MSH. The mean age is 42.85 +/- 23.94 years and 58% female.

2.3 Disease classification and clinical data processing

We used Clinical Classifications Software (CCS) tool, developed by Agency for Healthcare Research and Quality (AHRQ), which categorizes all diagnosis codes into a manageable number of clinically meaningful categories [9]. Each patient has been coded by ICD-9-CM or ICD-10-CM codes for their diagnosis at the time they visited hospital. CCS has two types of classifications, multi-level and single-level. The multi-level of CCS is used to group single-level CCS categories into broader body systems or condition categories (e.g., "Diseases of the Circulatory System", "Mental Disorders"). The multi-level system has four levels for diagnoses and we use the first level (N=18) to examine and assess disease enrichment by regions [9] .

We retrieved the zip codes based on patient home address in our EMR and removed the zip codes where the number of patients were less than 100 to ensure the data quality and validation. In this paper, the visualization by heat map is focus on NYC area and we reported the disease diagnosis rate, which was normalized against the total number of patients were seen in clinics in a specific zip code. Statistical analysis was performed on the whole population with surrounding neighborhood. The dataset was approved by IRB at Mount Sinai.

2.4 Environment data evaluation

The environmental data are collected from the Environmental Protection Agency (EPA) which are public available. The data are available in comma separated values (csv) since 2000. The data are reported with a time frequency of three days from 2000 to 2006 and each day was reported after 2006. The data is only available for 3 existing stations in New York City.

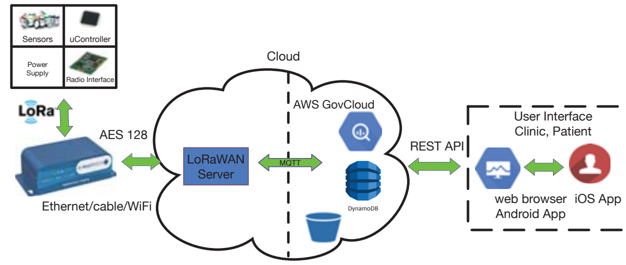

Figure 1. LoRaWAN Architecture.

2.5 A new wireless network architecture in New York

Nowadays, in the everyday life, the main purpose of the “things” is delimited to collect specific metrics without sharing and/or combine the data with other data streams, e.g., EMR. Thus, this kind of architecture can have several drawbacks. The device company owns the data and it exposes only a subset of the data collected. Due to lack in Application Programmable Interface, it can result difficulty to access to raw data (no post-processed data). The quality of sensors installed on the device can have a crucial impact on the data collected. An example can be constituted by the NetAtmo (https://www.netatmo.com) and Foobot (https://foobot.io/) devices, which are not able to retrieve indoor information without knowing the device owner granting the permission. A consequence of the issues above is the complexity of integrating the data from two or more different companies to create the right pool of data and new synthetic information. Apple tried to bypass this problem developing Health kit (https://developer.apple.com/healthkit), which can integrate the data collection from several fitness devices. However, only a subset of devices (e.g., Microsoft Band 2 is not allowed to use the App) have access to Health kit. The IoT device in our case would be easily configured and portable, as the end users do not necessary need to have access to personal wireless devices (i.e., smartphone or optimal WiFi coverage). Finally, the device allows the Plug and Play concept.

Therefore, we presented the LoRaWAN network that would leverages the location of the multiple clinics in the Mount Sinai health system to establish an IoT network around New York City and the 5 boroughs including Manhattan, the Bronx, Queens, Brooklyn, and Staten Island.

2.5.1 LoRaWAN network in Mount Sinai

We presented a wireless infrastructure (figure 1) creating an IoT architecture to solve the main problems of gathering data from high density sensors scenario with low bitrate.

The architecture features are as follows: scalability while more devices are present and the end-user device can be easily plugged and played (the only action required by the user is to turn on the device). At the other side, the network that exploits

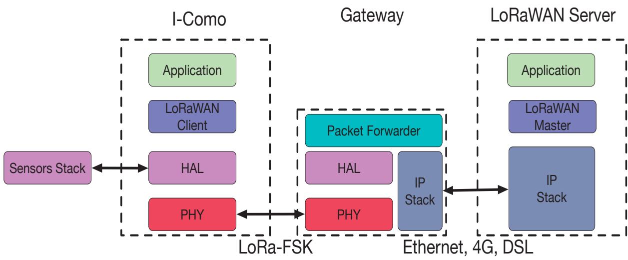

Figure 2. LoRaWAN protocol schema.

unlicensed frequency band would follow the Federal Communications Commission regulations.

The LoRa frequency in United States is between 902MHz to 928 MHz with 9 channels to downlink and 8 channels to uplink. Those frequencies allow to achieve a cover range of 2-5Km in urban scenario and up to 15 Km in suburban area. The LoRaWAN protocol schema is reported in Figure 2. LoRaWAN network and architecture is typically laid out in a star-of-stars topology, where gateway is a transparent bridge relaying messages between nodes and a central network server in the cloud. Gateway is connected to the network server via standard IP connections while end-user devices use single-hop wireless communication to one or many gateways. All nodes communication is generally bi-directional, and support operation such as multicast enabling software upgrade as well [10]. For more details see https://www.lora-alliance.org.

This architecture routing all data package in a cloud system is called LoRaWAN server. This device retrieves the information through the Message Queue Telemetry Transport Protocol (MQTT) and updates the Amazon Web Services (AWS) cloud to store the data in redundant encrypted data storage. To ensure data security and privacy, LoRa provides additional security measures, which makes the devices more robust. Although the data shared between the LoRA gateway and AWS is still bound by the inherent security flaws of other devices, the sensitive data being transmitted from the environmental sensors can be encrypted in both directions using LoRa Security protocols. The LoRaWAN protocol requires that packets of information are both signed and encrypted before transmission. These tasks are completed using symmetric keys known both to the Node and to the Network Server. They are also distributed in one of two ways depending on how a Node joins the network; Over-The-Air-Activation (OTAA) and Activation be Personalization (ABP) [11]. Additionally, the data can be mixed with additional information gathered from other data stream as EMR. We can use machine learning techniques as Deep Learning through the Deep Patient [8] framework to create useful knowledge hospital exploiting spatial and temporal information for both end users and hospitals. Therefore, with LoRaWAN having all the data on AWS and data encryption is intrinsically made inside its features. Furthermore, exploiting the multiple locations of Mount Sinai network (Figure 3) allows us to place several LoRaWan gateways around the city and the 5 boroughs. Therefore, a single gateway LoRaWan is feasible to cover a few city blocks by increasing the gateways density and has a better coverage in term of distance and number of messages exchanged between nodes and gateways.

Figure 3. Mount Sinai clinics in Manhattan, Queens and Brooklyn.

2.5.2 I-Como

The last part of the architecture is represented by the user device. The name is I-Como from IoT-Como. This device has features that can be plugged and played on the outlet without any user interaction. Consistent with the federal Health Insurance Portability and Accountability Act (HIPAA), we will ask users' permission to receive ownership of, use and share that information. Many features in LoRaWAN are the wide range. Users can avoid pairing the device as the messages are directly gathered from the gateways placed in the Mount Sinai clinics. Moreover, due to the low power of the LoRa radio, I-Como is designed to support a small lithium battery and a BLE transceiver to allow mobility and pair I-Como with other devices already in the patient life. An example can be any heart rate device, which uses BLE exposing its service with the standard hex-code representation. In such way, the I-Como can be a gateway that can piggyback other data from third party devices. The I-Como hardware characteristics are: ARM-M0 microcontroller, LoRa and BLE radio transceiver, and a 1000mAh lithium-battery. The sensors part is composed by: light [Lux], noise [Db], temperature [C/F], relative humidity [%], pressure [mbar], and PM 2.5 [μg/m3]. The device is expandable through Serial Peripheral Interface (SPI) with a daughter board featuring carbon monoxide (CO)[ppm], ozone (O3), sulfur dioxide (SO2) [ppm] and nitrogen dioxide (NO2) [ppm]. All the chemical quantities are the most frequent gases made by a fossil fuel engine.

Location*	ZipCode	Metrics	2005	2006	2007	2008	2009	2010	2011	2012	2013	2014	2015	2016
Circulatory System														
UM	10033	Rate(%)	10.18	12.33	26.57	29.39	26.67	33.43	44.29	43.98	40.05	41.69	35.69	30.33
		P Fisher	0.0002	0.0003	0.0007	6E-06	0.0094	2E-13	2E-32	2E-28	2E-17	4E-23	1E-11	0.2231
	10040	Rate(%)	13.44	15.76	21.84	25.23	22.04	30.99	44.88	43.61	42.95	41.33	33.65	25.92
		P Fisher	0.1083	0.1414	0.4615	0.0886	0.6164	6E-07	3E-28	2E-23	3E-22	9E-16	0.0005	0.0006
Endocrine; nutritional; and metabolic diseases and immunity disorders														
UM	10033	Rate(%)	8.14	13.45	16.73	25.49	23.33	28.20	40.92	41.49	38.61	36.36	33.42	31.08
		P Fisher	0.019	0.5023	0.541	0.0051	0.0477	1E-05	1E-22	5E-20	6E-11	0.0017	0.2108	0.6155
	10040	Rate(%)	11.80	12.50	14.56	23.22	18.83	26.20	41.10	38.09	41.12	38.91	32.12	27.21
		P Fisher	1	0.2677	0.5422	0.2274	0.2761	0.011	5E-19	4E-09	2E-14	4E-07	0.633	1E-05
Respiratory System														
EH	11029	Rate(%)	21.69	22.85	27.99	29.08	30.17	21.90	30.64	34.89	35.07	33.76	29.98	29.94
		P Fisher	1E-91	4E-106	6E-192	7E-187	6E-171	1E-54	6E-171	1E-289	9E-292	1E-297	5E-215	2E-101
	11035	Rate(%)	19.42	20.49	26.19	29.75	32.25	24.67	30.95	33.36	34.04	32.59	29.79	31.13
		P Fisher	2E-07	5E-09	8E-24	6E-35	1E-78	7E-32	6E-45	3E-59	3E-69	5E-66	2E-60	2E-42
Neoplasms														
BYN	11234	Rate(%)	1.60	5.38	6.53	8.04	8.25	8.47	15.97	12.29	13.13	19.02	16.53	15.84
		P Fisher	0.7608	0.0012	0.0008	0.0001	2E-05	0.0065	3E-06	0.0167	6E-05	4E-13	2E-11	5E-08
M	11022	Rate(%)	3.11	3.90	4.23	5.26	6.16	7.11	12.20	10.98	12.09	15.42	14.15	14.95
		P Fisher	0.0073	0.002	0.0229	0.0284	0.0004	0.0446	0.0628	0.168	0.0002	9E-07	1E-06	2E-09
UW	11023	Rate(%)	2.47	3.09	4.62	7.06	6.09	6.32	11.77	11.99	10.79	14.42	12.88	11.76
		P Fisher	0.0173	0.0063	7E-05	2E-11	8E-07	0.2169	0.0568	8E-05	0.0092	2E-08	8E-06	0.005
Genitourinary System														
M	11019	Rate(%)	8.56	8.63	11.56	11.69	10.62	14.06	17.89	19.50	20.54	37.41	29.54	22.80
		P Fisher	0.5542	0.674	0.6011	0.9542	0.1009	0.964	0.0308	0.5802	0.7109	5E-93	9E-39	8E-05
UW	11023	Rate(%)	8.50	9.26	11.18	11.70	12.84	15.43	21.06	21.83	21.49	29.17	26.68	24.01
		P Fisher	0.3744	0.916	0.7069	0.9137	0.4708	0.031	0.2941	0.0091	0.0307	3E-27	3E-26	5E-14

Table 1 * UM: Upper Manhattan; BYN: Brooklyn; M: Midtown; UW: Upper West; EH: East Harlem.

3 RESULTS AND DISCUSSION

3.1 Diagnosis rate for environmental diseases

We have 487 zip codes remaining with at least 100 unique patient records in our dataset. We investigated disease diagnosis rates for each zip code for all 18-disease categories. We used Environmental Diseases from A-Z published by National Institute of Environmental Health Sciences (NIEHS) as a guideline to analyze diseases impacted by environmental factors [12] in our cohort. We investigated 5 disease categories reported as environmental diseases including 'diseases of the circulatory system' (DCS), 'endocrine; nutritional; and metabolic diseases and immunity disorders' (ENMI), 'diseases of the respiratory system' (DRS), 'diseases of the genitourinary system' (DGS), and 'neoplasms' (CA). We also investigated 'diseases of the digestive system' (DDS) as a control. The average diagnosis rate were 26%, 25%, 22%, 16%, 7%, and 19% for DCS, ENMI, DRS, DGS, CA and DGS respectively across 2005-2016.

3.2 Differential disease enrichments specific to geographic regions

We performed disease enrichment analysis for 30 zip codes in NYC area. We identified significantly differential disease enrichment patterns for zip codes. For instance, DCS and ENMI were significantly enriched in zip codes categorized as upper Manhattan, Queens, and Brooklyn particularly after 2010 ($p<0.0001$, Table 1), while DRS was significantly enriched in zip codes categorized as east Harlem and central Harlem ($p<0.0001$, Figure 6, Table 1). Neoplasms was significantly enriched in zip codes categorized as mid-town, upper west, and Brooklyn particularly after 2010 and 2013 ($p<0.0001$, Figure 6, Table 1). Similarly, DGS was significantly enriched in mid-town, upper west, as well as upper Manhattan after 2013 ($p<0.0001$, Figure 6, Table 1). Interestingly, there is no significant difference for DDS across the zip codes in NYC area. The findings demonstrated that environmental diseases were influenced on our geographically different patient population. Furthermore, data from the United States Census Bureau data demonstrates that residents in zip codes enriched with DCS, ENMI and DRS represent the lowest socioeconomic class in New York state with a median household income of $27,424-$46,200 (versus a median household income of $58,003 for the state of New York). In addition, the high school graduation rate is lower in these zip codes than New York State average (65.2%-75.5% vs. 85.2%) (https://factfinder.census.gov). This could also potentially infer that these residents in these areas could carry Affordable Care Act from 2010 March due to low income, and it may explain the sudden increased diagnosis rate for DRS, DCS and ENMI, underlying the under-diagnosis rate prior to 2010 for those patients. DRS was solely enriched in east Harlem and its neighborhood areas, may potentially be affected by the pollution such as bio-aerosols from the wastewater treatment plant in the same area, ranking the 2nd largest wastewater treatment plant in NY, and many studies have shown that respiratory diseases were associated with bio-aerosols, bacteria, and fungi emitted from wastewater treatment plant [13-16].

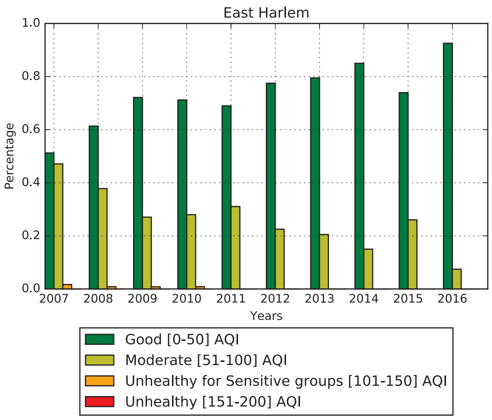

Figure 4 Air Quality Index in Upper West station

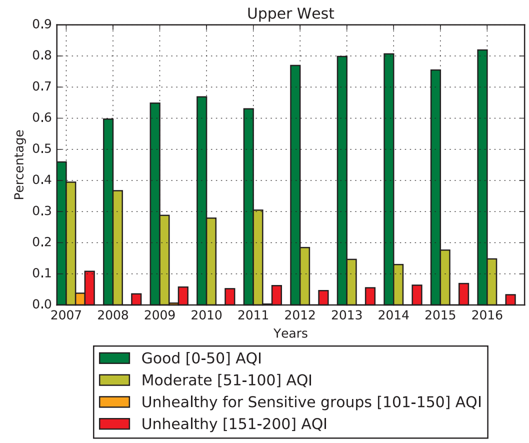

Figure 5. Air Quality Index in Upper West station

3.3 Environmental impact

We computed the percentage of days classified with the Air Quality Index (AQI) from two air pollution stations in East Harlem and in west part of Manhattan (Figure 4 and Figure 5), with distance around 2 miles between two stations. The other data collected are Particular Matter (PM) 2.5 [$\mu g/m^3$], temperature [C], Ozone [ppm], and humidity [%]. The percentage of days with a good air (0-50) was increased for the entire time frame, but with a slight difference between the two stations, while more unhealthy days were observed in the west part. Unhealthy AQI (>150) was significant higher in upper east compared with east Harlem ($p<0.0001$), and the significance persists for unhealthy AQI for sensitive group (>100) in upper part ($p=0.0002$), which may explain the enrichment for neoplasm and genitourinary systems in upper east and midtown areas (Figure 4-6). There is no significant difference for these areas compared to NYC average for socioeconomic status, high school graduation level, and median household income. The zip codes are sorted from bottom to top to represent lower Manhattan, midtown, upper east, upper west, Harlem and upper Manhattan in Figure 6. This scenario opens interesting challenges in collection data sensors where the patients live. e.g. air pollution, water pollution (e.g, CO, SO2, NO2, O3)

4 CONCLUSIONS

We presented a data-driven approach to identify geographic patterns of environmental diseases using EMR and EPA data. Our analysis found different geographic areas in NYC enriched with specific disease categories. These results suggest that the environment factors could be potentially measured as a customized device and at a granular basis based on geographic disease differences. We plan to extend this work in future studies to consider the key drivers/disease in each disease category affected by environment and comparison for all zip codes across the NYC neighborhood. The objective is to create a LoRaWAN architecture to deploy a granular IoT network collecting indoor data and data from vast of sensors to help to understand the disease trend. We could create an artificial intelligence agent based on several and heterogeneous data streams (air and water pollution, life style, medical records). This element could be integrated to create a new index representing the patient health status in order to improve the patients' quality of life.

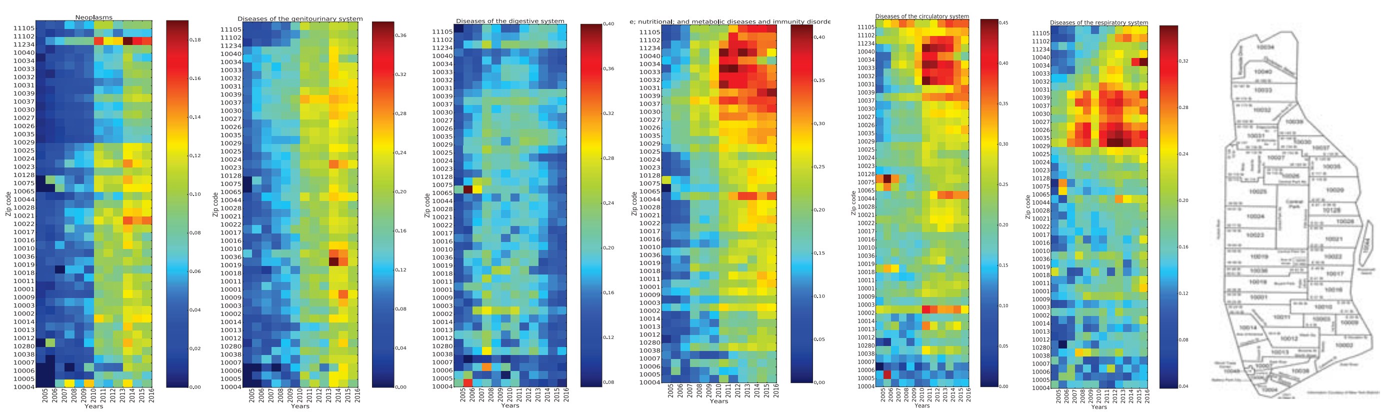

Figure 6 Manhattan zip code map and 5 environmental diseases and 1 disease as a control

REFERENCES

[1] Xu, X., Wang, G., Chen, N., Lu, T., Nie, S., Xu, G., Zhang, P., Luo, Y., Wang, Y., Wang, X., Schwartz, J., Geng, J. and Hou, F. F. Long-Term Exposure to Air Pollution and Increased Risk of Membranous Nephropathy in China. *J Am Soc Nephrol*, 27, 12 (Dec 2016), 3739-3746.

[2] Brook, R. D., Franklin, B., Cascio, W., Hong, Y., Howard, G., Lipsett, M., Luepker, R., Mittleman, M., Samet, J., Smith, S. C., Jr., Tager, I., Expert Panel on, P. and Prevention Science of the American Heart, A. Air pollution and cardiovascular disease: a statement for healthcare professionals from the Expert Panel on Population and Prevention Science of the American Heart Association. *Circulation*, 109, 21 (Jun 01 2004), 2655-2671.

[3] Bruno, R. M., Di Pilla, M., Ancona, C., Sorensen, M., Gesi, M., Taddei, S., Munzel, T. and Virdis, A. Environmental factors and hypertension. *Curr Pharm Des* (Mar 21 2017).

[4] Nel, A. Atmosphere. Air pollution-related illness: effects of particles. *Science*, 308, 5723 (May 06 2005), 804-806.

[5] Raaschou-Nielsen, O., Pedersen, M., Stafoggia, M., Weinmayr, G., Andersen, Z. J., Galassi, C., Sommar, J., Forsberg, B., Olsson, D., Oftedal, B., Krog, N. H., Aasvang, G. M., Pyko, A., Pershagen, G., Korek, M., De Faire, U., Pedersen, N. L., Ostenson, C. G., Fratiglioni, L., Sorensen, M., Eriksen, K. T., Tjonneland, A., Peeters, P. H., Bueno-de-Mesquita, H. B., Plusquin, M., Key, T. J., Jaensch, A., Nagel, G., Foger, B., Wang, M., Tsai, M. Y., Grioni, S., Marcon, A., Krogh, V., Ricceri, F., Sacerdote, C., Migliore, E., Tamayo, I., Amiano, P., Dorronsoro, M., Sokhi, R., Kooter, I., de Hoogh, K., Beelen, R., Eeftens, M., Vermeulen, R., Vineis, P., Brunekreef, B. and Hoek, G. Outdoor air pollution and risk for kidney parenchyma cancer in 14 European cohorts. *Int J Cancer*, 140, 7 (Apr 01 2017), 1528-1537.

[6] E. Menegatti, M. D., M. Mina, A. Pretto, A. Bardella, S. Zanconato, P. Zanuttigh, A. Zanella Autonomous discovery, localization and recognition of smart objects through WSN and image features. *2010 IEEE Globecom Workshops* (2010).

[7] Li, L., Boland, M. R., Miotto, R., Tatonetti, N. P. and Dudley, J. T. Replicating Cardiovascular Condition-Birth Month Associations. *Sci Rep*, 6 (Sep 14 2016), 33166.

[8] Miotto, R., Li, L., Kidd, B. A. and Dudley, J. T. Deep Patient: An Unsupervised Representation to Predict the Future of Patients from the Electronic Health Records. *Sci Rep*, 6 (May 17 2016), 26094.

[9] Cowen, M. E., Dusseau, D. J., Toth, B. G., Guisinger, C., Zodet, M. W. and Shyr, Y. Casemix adjustment of managed care claims data using the clinical classification for health policy research method. *Med Care*, 36, 7 (Jul 1998), 1108-1113.

[10] Nicola Bui, M. R., Cristiano Tapparello, Michele Zorzi Reprogramming over the Air and Sensor Island Management through SYNAPSE++. *IEEE* (2009).

[11] Miller, R. LoRa Security: Building a Secure LoRa Solution. *MWR Labs Whitepaper* (2016).

[12] US Department of Health and Human Services, N. I. o. E. H. S., National Institutes of Health Environmental Diseases from A to Z. *NIH Publication No. 96-4145*, Second Edition (2007).

[13] Cyprowski, M., Sowiak, M., Soroka, P. M., Buczyrnska, A., Kozajda, A. and Szadkowska-Stanczyk, I. [Assessment of occupational exposure to fungal aerosols in wastewater treatment plants]. *Med Pr*, 59, 5 (2008), 365-371.

[14] Jahangiri, M., Neghab, M., Nasiri, G., Aghabeigi, M., Khademian, V., Rostami, R., Kargar, V. and Rasooli, J. Respiratory disorders associated with occupational inhalational exposure to bioaerosols among wastewater treatment workers of petrochemical complexes. *Int J Occup Environ Med*, 6, 1 (Jan 2015), 41-49.

[15] Seetha, N., Bhargava, R. and Gurjar, B. R. Gaseous and bioaerosol emissions from municipal wastewater treatment plants. *J Environ Sci Eng*, 55, 4 (Oct 2013), 517-536.

[16] Shiryaeva, O., Aasmoe, L., Straume, B., Olsen, A. H., Ovrum, A., Kramvik, E., Larsen, M., Renstrom, A., Merritt, A. S., Heldal, K. K. and Bang, B. E. Respiratory effects of bioaerosols: exposure-response study among salmon-processing workers. *Am J Ind Med*, 57, 3 (Mar 2014), 276-285.